SARS-CoV-2 Encodes a PPxY Late Domain Motif that is Known to Enhance Budding and Spread in Enveloped RNA Viruses

Halim Maaroufi
Institut de biologie intégrative et des systèmes (IBIS). Université Laval. Québec. Canada
Halim.maaroufi@ibis.ulaval.ca

ABSTRACT Currently, the global COVID-19 (Coronavirus Disease-2019) pandemic is affecting the health and/or socioeconomic live of almost each people in the world. Finding vaccines and therapeutics is urgent but without forgetting to elucidate the molecular mechanisms that allow some viruses to become dangerous for humans. Here, analysis of all proteins of SARS-CoV-2 revealed a unique PPxY Late (L) domain motif ^{25}PPAY^{28} in spike protein inside hot disordered loop predicted subject to phosphorylation and binding. It was demonstrated in enveloped RNA viruses that PPxY motif recruits Nedd4 E3 ubiquitin ligases and ultimately the ESCRT complex to enhance virus budding and release that means a high viral load, thus facilitating new infections. Note that PPxY motif is not present in proteins of SARS-CoV. This suggests that PPxY motif by its role in enhancing the viral load could explain why SARS-CoV-2 is more contagious than SARS-CoV. Of course, after the experimental verifications showing that PPxY motif plays the same role as reported for other enveloped RNA viruses, it could become an interesting target for the development of novel host-oriented antivirals therapeutics for preventing S protein to recruit Nedd4 E3 ligases partners.

KEYWORDS SARS-CoV-2; Spike protein; PPxY Late Domain Motif; WW-domain; Nedd4 E3 ubiquitin ligases; Budding; Spread

INTRODUCTION

Currently, the global COVID-19 (Coronavirus Disease-2019) pandemic caused by SARS-CoV-2 from Wuhan is affecting the health (including psychology) and/or socioeconomic of almost each citizen in the world. Finding vaccines and therapeutics to fight CoV-2 is urgent. In addition, it is necessary to continue this great research effort in the next years to elucidate the molecular mechanisms (tropism, cell penetration, multiplication and spread, etc) that emerging viruses (now SARS-CoV-2) use to infect humans. This knowledge is an investment for the future to prevent and/or controle emergence of dangerous viruses that may be will be more terrible for humanity than SARS-CoV-2. The family of coronaviruses (CoVs) is large and composed of single positive-stranded enveloped RNA viruses (Graham and Baric, 2010; Li, 2013). Among all RNA viruses, CoVs possess the largest genome, typically between 27.000 and 32.000 nucleotides. They are classified into Alpha-, Beta-, Gamma-, and Deltacoronavirus genetic genera and can infect both mammalian and avian species. SARS-CoV-2 is more to SARS-CoV than MERS-CoV, but all belong to betacoronavirus (betaCoVs) (de Wit et al., 2016).

The envelope-anchored SARS-CoV-2 spike (S) is a multifunctional glycoprotein with 1273 amino acid residues. Its structure was resolved as a homotrimeric with several domains. S protein is subdivided into S1 and S2 subunits. S1 is formed by two domains, an N-terminal domain (NTD) and a C-terminal receptor-binding domain (RBD) that binds specifically the host receptor angiotensin-converting enzyme 2 (ACE2) on the host cell surface (Li, 2012). Whereas, S2 subunit is also multidomains and induces viral and host membranes fusion.

The viral proline-rich Pro–Pro-x-Tyr (PPxY) Late or L- domain motif (Chen and Sudol, 1995) interacts with host proteins containing WW-domain. The term Late reflects late function in virus lifecycle (Freed, 2002). L-domain motifs are identified in enveloped RNA viruses such as in Gag of number of retroviruses and in matrix of arenaviruses, rhabdoviruses and filoviruses (Baillet et al., 2019; Bieniasz, 2006; Wirblich et al., 2008). WW-domain is a small domain of 35–40 amino acids, named after two conserved tryptophan (W) residues in the sequence (Bork and Sudol, 1994). It is a fold of three-stranded antiparallel β-sheet that contains two ligand-binding grooves (Huang et al., 2000; Kanelis et

al., 2001). RNA viruses' proteins use PPxY L-domain motif to recruit specific WW-domain of host proteins of either Nedd4 (Neuronal precursor cell-Expressed Developmentally Down-regulated 4), or Nedd4 family members to facilitate their egress and spread (Bieniasz, 2006). Nedd4 proteins family have three domains, N-terminal lipid binding (C2) domain; WW modules, present in multiple copies; and a C-terminal Hect (for homologous to E6-associated protein C terminus) domain that contains the ubiquitin ligase activity.

Previous and current works are focusing to understand the first step that allows SARS-CoV and SARS-CoV-2 penetrate host cell. Principally, these works are studying interaction between C-terminal receptor-binding domain (RBD) of S protein and the host receptor angiotensin-converting enzyme 2 (ACE2). Here, molecular mechanism of the last step (late function virus life cycle) of budding and release of virus is presented. The N-terminal of SARS-CoV-2 spike protein contains a PPxY L-domain motif that is known to hijack host WW-domain of Nedd4 E3 ubiquitin ligases and ultimately the ESCRT (Endosomal Sorting Complex Required for Transport) complex to enhance virus budding and spread. Importantly, this motif is absent in SARS-CoV that could explain why SARS-CoV-2 is more contagious than SARS-CoV. Developing a novel host-oriented inhibitor of molecular interactions of PPxY–host WW-domain will be welcome to fight SARS-CoV-2 infection.

RESULTS AND DISCUSSION

The N-terminal of S protein contains a PPxY L-domain motif

Sequence analysis of SARS-CoV-2 spike protein by the eukaryotic linear motif (ELM) resource (http://elm.eu.org/) revealed a short linear motif (SLiMs) known as PPxY Late (L-) domain motif, ^{25}PPAY^{28} in N-terminal of S1 subunit. PPxY L-domain motif interacts with proteins containing WW-domain (s). The term Late reflects late function in virus lifecycle (Freed, 2002). L-domain motifs were identified in single stranded enveloped RNA viruses (Table 1). In Gag protein of number of retroviruses and in matrix of arenaviruses, rhabdoviruses and filoviruses (Baillet et al., 2019; Bieniasz, 2006; Wirblich et al., 2008). RNA viruses use PPxY L-domain motif to recruit specific WW-domain of host proteins of Nedd4 family members and ultimately the ESCRT complex to facilitate their budding and egress (Bieniasz, 2006). Interestingly, SARS-CoV-2 S protein and Nedd4 can be S-palmitoylated, suggesting that they can be localize to similar membrane subdomains (Petit et al., 2007; Gordon et al., 2020; Chesarino et al., 2014). Therefore, they could be able to interact. In addition, ScanProsite tool (https://prosite.expasy.org/scanprosite/) is used to verify if PPxY motif is present elsewhere in SARS-CoV-2 and SARS-CoV proteins. PPxY motif is absent in SARS-CoV and only present in S protein of SARS-CoV-2. It was demonstrated in enveloped RNA viruses that PPxY motif recruits Nedd4 E3 ubiquitin ligases and ultimately the ESCRT complex to enhance virus budding and release that means a high viral load, thus facilitating new infections. Note that PPxY motif is not present in proteins of SARS-CoV. This suggests that PPxY motif by its role in enhancing the viral load could explain why SARS-CoV-2 is more contagious than SARS-CoV (To et al., 2020).

PPxY motif is also present in S protein of bat RaTG13and pangolin GX-P5L (Fig. 1A). Note that S proteins with PPxY motif are phylogenetically close (Fig. 1C). Interestingly, alignment of S protein sequences of the two pangolins showed only two differences in S1 subunit (amino acid in position 25 (P/Q) and deletion of ^{448}GY^{449} in pangolin GX-P1E) (Lam et al., 2020; Zhang et al., 2020). In the future, it would be interesting to compare pathogenicity of pangolin GX-P1E and pangolin GX-P5L coronaviruses to know if the loss of PPxY motif is important for pathogenicity. Figure 1B shows the difference in

coronaviruses counterpart nucleotides of codon Pro25 of SARS-CoV-2. It has been noticed that mutations are more probable at second and third nucleotide base of a codon than at the first nucleotide base. Therefore, it is more probable that mutation from Gln (CAG) to Pro (CCG) occurs than Ala (GCT) to Proline (CCT). Moreover, a mutation is less probable from Asn (AAT) to Proline (CCT) (Fig. 1B). May be this explains why SARS-CoV mutations have not (yet) given birth to PPxY motif.

PPxY L-domain motif is in hot region

Scanning SARS-CoV-2 S protein sequence with DisEMBL software (Linding et al., 2003) revealed in the N-terminal region a unique hot disordered loop ^{19}TTRTQL**PP**A**Y**TNSFT^{33} that includes PPxY motif (Table 2). In addition, this loop contains other motifs. Indeed, PPxY motif shares its tyrosine with an overlapping ^{28}YTNSF^{32} motif (Fig. 1A) that when its Tyr28 is phosphorylated it allows binding of STAP1 SH2 domain. STAP1 (Signal Adaptor Protein 1) is an adaptor protein with an SH2 and a PH class of lipid-binding domain (Wang et al., 1994). It is expressed in lymphoid cells and is phosphorylated by the Tec tyrosine kinase (Tec TK), which participates in B cell antigen receptor signaling (Ohya et al., 1999; Yang et al., 2001). It has been showed in polyoma virus that when its middle T-antigen is phosphorylated on tyrosine, it acts as a binding site for the SH2 domain of phosphatidylinositol-3'OH kinase 85K subunit (Dilworth et al. 1994). Another site, ^{28}YTNS^{31} in S protein is also Tyr phosphorylation depending for binding STAT5 SH2 domain (Lin et al., 2006).

The hot region in S protein contains also Ser/Thr phosphorylated motifs. Indeed, PPxY motif shares also its Pro25 with an overlapping ^{19}TTRTQL**P**^{25} that could be phosphorylated at TQ motif by Phosphatidylinositol 3- and/or 4-kinase (PIKKs). The Gln (Q) beside to the target Ser/Thr is critical for the substrate recognition. PIKKs are Ser/Thr atypical kinases that are found only in eukaryotes (Imseng et al., 2108; Angira et al., 2020). Interestingly, Yang et al. (2012) showed that phosphatidylinositol 4-kinase IIIβ (PI4KB) is required for cellular entry by pseudoviruses bearing the SARS-CoV S protein. This cell entry is highly inhibited by knockdown of PI4KB. Moreover, they demonstrated that PI4KB does not affect virus entry at the SARS-CoV S-ACE2 interface. Finally, ^{26}PAY**T**NSF**T**^{33} is recognised by Ser/Thr kinase GSK3 (Glycogen synthase kinase 3). Interestingly, it was

reported that the lipid kinase phosphatidylinositol 4-kinase II α (PI4KIIα) is a substrate of GSK3 (Robinson et al. 2014). This establishes a link with ^{19}TTRTQL**P**^{25}motif, described above, that is predicted phosphorylated by GSK3.

Interactions of PPxY L-domain motif with Nedd4-WW3-domain Ub ligase

In the aim to compare the interactions of PPAY S protein-Nedd4WW-domain with other complexes of PPxY-Nedd4WW-domain, molecular docking was performed with the software AutoDock vina (Trott and Olson, 2010). Fig. 2 shows that ^{23}QL**PP**A**Y**TNS^{31} peptide of SARS-CoV-2 S protein is localized in the same region as ^{23}QL**PP**A**Y**TNS^{31} of Zaire Ebola virus Matrix protein VP40 (PDBid: 2KQ0) and important amino acids of ^{23}QL**PP**A**Y**TNS^{31} peptide are superposed with those of Ebola VP40 peptide, except the orientation of aromatic cycle of tyrosine (Fig. B and C). Iglesias-Bexiga et al. (2019) noticed that Nedd4-WW3 binding site is highly plastic and that can accommodate PPxY-containing ligands with varying orientations. This structural superposition with PPxY of VP40 confirmed the reliability of AutoDock vina peptide docking module. Knowing molecular interactions of ^{23}QL**PP**A**Y**TNS^{31} and Nedd4WW-domain will help to design a peptide able to mimic the surface of Nedd4 WW-domain and that will strongly bind to ^{23}QL**PP**A**Y**TNS^{31} peptide preventing the recruitment of Nedd4 E3 ubiquitin ligase by SARS-CoV-2 S protein (Zaidman and Wolfson, 2016). Indeed, Han et al. (2014) have developed two lead compounds that specifically block the VP40 PPxY-host Nedd4 interaction with an antibudding activity into the nanomolar range.

MATERIALS AND METHODS

Sequence analysis

To search probable short linear motifs (SLiMs), SARS-CoV-2 spike protein sequence was scanned with the eukaryotic linear motif (ELM) resource (http://elm.eu.org/). PPxY L-domain motif was searched in proteins of SARS-CoV-2 and SARS-CoV using https://prosite.expasy.org/scanprosite/

3D modeling and molecular docking

Unfortunately, the region containing ^{23}QL**PP**A**Y**TNS^{31}peptide has not been resolved in all known structures of spike S protein. So, Pep-Fold (Thevenet et al., 2012) software was used to model *de novo* this peptide. The model quality of the peptide was assessed by analysis of a Ramachandran plot through PROCHECK (Vaguine et al., 1999).

The docking of the peptide into human Nedd4 3rd WW-domain (PDBid: 2KQ0_A) was performed with the software AutoDock vina (Trott and Olson, 2010). The 3D complex containing Human Nedd4 3rd WW-domain and peptide was refined by using FlexPepDock (London et al., 2011), which allows full flexibility to the peptide and side-chain flexibility to the receptor. The electrostatic potential surface of the B56 subunit was realized with PyMOL software (http://pymol.org/).

Phylogeny

Amino acid residues sequences of spike (S) protein of SARS-CoV-2 (accession: YP_009724390.1), SARS-Cov (P59594.1), bat_coronavirus_RaTG13 (QHR63300.2), pangolin_PCoV_GX-P5L (QIA48632.1), pangolin_PCoV_GX-P1E (QIA48623.1), bat_CoVZC45_CoV (AVP78031.1) and bat_Rs4874_CoV (ATO98205.1), were aligned with T-coffee software (Rius et al., 2011). This multiple alignment is used to establish the phylogenetic relationships between SARS-CoV-2 and others coronaviruses. The phylogenetic tree was constructed with MrBayes (Huelsenbeck and Ronquist, 2001) using: Likelihood model (Number of substitution types: 6(GTR); Substitution model: Poisson; Rates variation across sites: Invariable + gamma); Markov Chain Monte Carlo parameters (number of generations: 100 000; Sample a tree every: 1000 generations) and Discard first 500 trees sampled (burnin).

ACKNOWLEDGMENTS

I would like to thank the IBIS bioinformatics group for their assistance.

CONFLICT OF INTERESTED

The author declares that he has no conflicts of interest.

REFERENCES

Angira, D., Shaik, A., Thiruvenkatam, V., 2020. Structural and strategic landscape of PIKK protein family and their inhibitors: an overview. Front. Biosci. 25, 1538–1567.

Baillet, N., Krieger, S., Carnec, X., Mateo, M., Journeaux, A., Merabet, O., Caro, V., Tangy, F., Vidalain, P.-O., Baize, S., 2019. E3 Ligase ITCH Interacts with the Z Matrix Protein of Lassa and Mopeia Viruses and Is Required for the Release of Infectious Particles. Viruses 12. https://doi.org/10.3390/v12010049

Bieniasz, P.D., 2006. Late budding domains and host proteins in enveloped virus release. Virology 344, 55–63. https://doi.org/10.1016/j.virol.2005.09.044

Bork, P., Sudol, M., 1994. The WW domain: a signalling site in dystrophin? Trends Biochem. Sci. 19, 531–533. https://doi.org/10.1016/0968-0004(94)90053-1

Bouamr, F., Melillo, J.A., Wang, M.Q., Nagashima, K., de Los Santos, M., Rein, A., Goff, S.P., 2003. PPPYVEPTAP motif is the late domain of human T-cell leukemia virus type 1 Gag and mediates its functional interaction with cellular proteins Nedd4 and Tsg101 [corrected]. J. Virol. 77, 11882–11895. https://doi.org/10.1128/jvi.77.22.11882-11895.2003

Chen, H.I., Sudol, M., 1995. The WW domain of Yes-associated protein binds a proline-rich ligand that differs from the consensus established for Src homology 3-binding modules. Proc. Natl. Acad. Sci. U. S. A. 92, 7819–7823. https://doi.org/10.1073/pnas.92.17.7819

Chesarino, N.M., Hach, J.C., Chen, J.L., Zaro, B.W., Rajaram, M.V., Turner, J., Schlesinger, L.S., Pratt, M.R., Hang, H.C., Yount, J.S., 2014. Chemoproteomics reveals Toll-like receptor fatty acylation. BMC Biol. 12, 91. https://doi.org/10.1186/s12915-014-0091-3

de Wit, E., van Doremalen, N., Falzarano, D., Munster, V.J., 2016. SARS and MERS:

recent insights into emerging coronaviruses. Nat. Rev. Microbiol. 14, 523–534. https://doi.org/10.1038/nrmicro.2016.81

Dilworth, S.M., Brewster, C.E., Jones, M.D., Lanfrancone, L., Pelicci, G., Pelicci, P.G., 1994. Transformation by polyoma virus middle T-antigen involves the binding and tyrosine phosphorylation of Shc. Nature 367, 87–90. https://doi.org/10.1038/367087a0

Dolnik, O., Kolesnikova, L., Stevermann, L., Becker, S., 2010. Tsg101 is recruited by a late domain of the nucleocapsid protein to support budding of Marburg virus-like particles. J. Virol. 84, 7847–7856. https://doi.org/10.1128/JVI.00476-10

Freed, E.O., 2002. Viral late domains. J. Virol. 76, 4679–4687. https://doi.org/10.1128/jvi.76.10.4679-4687.2002

Graham, R.L., Baric, R.S., 2010. Recombination, reservoirs, and the modular spike: mechanisms of coronavirus cross-species transmission. J. Virol. 84, 3134–3146. https://doi.org/10.1128/JVI.01394-09

Gordon, D.E., Jang, G.M., Bouhaddou, M., Xu, J., Obernier, K., O'Meara, M.J., Guo, J.Z., Swaney, D.L., Tummino, T.A., Huettenhain, R., Kaake, R.M., Richards, A.L., Tutuncuoglu, B., Foussard, H., Batra, J., Haas, K., Modak, M., Kim, M., Haas, P., Polacco, B.J., Braberg, H., Fabius, J.M., Eckhardt, M., Soucheray, M., Bennett, M.J., Cakir, M., McGregor, M.J., Li, Q., Naing, Z.Z.C., Zhou, Y., Peng, S., Kirby, I.T., Melnyk, J.E., Chorba, J.S., Lou, K., Dai, S.A., Shen, W., Shi, Y., Zhang, Z., Barrio-Hernandez, I., Memon, D., Hernandez-Armenta, C., Mathy, C.J.P., Perica, T., Pilla, K.B., Ganesan, S.J., Saltzberg, D.J., Ramachandran, R., Liu, X., Rosenthal, S.B., Calviello, L., Venkataramanan, S., Liboy-Lugo, J., Lin, Y., Wankowicz, S.A., Bohn, M., Sharp, P.P., Trenker, R., Young, J.M., Cavero, D.A., Hiatt, J., Roth, T.L., Rathore, U., Subramanian, A., Noack, J., Hubert, M., Roesch, F., Vallet, T., Meyer, B., White, K.M., Miorin, L., Rosenberg, O.S., Verba, K.A., Agard, D., Ott, M., Emerman, M., Ruggero, D., García-Sastre, A., Jura, N., von Zastrow, M., Taunton, J., Ashworth, A., Schwartz, O., Vignuzzi, M., d'Enfert, C., Mukherjee, S., Jacobson, M., Malik, H.S., Fujimori, D.G., Ideker, T., Craik, C.S., Floor, S., Fraser, J.S., Gross, J., Sali, A., Kortemme, T., Beltrao, P., Shokat, K., Shoichet, B.K., Krogan, N.J., 2020. A SARS-CoV-2-Human Protein-Protein Interaction Map Reveals Drug Targets and Potential Drug-Repurposing. bioRxiv. https://doi.org/10.1101/2020.03.22.002386

Han, Z., Lu, J., Liu, Y., Davis, B., Lee, M.S., Olson, M.A., Ruthel, G., Freedman, B.D., Schnell, M.J., Wrobel, J.E., Reitz, A.B., Harty, R.N., 2014. Small-molecule probes

targeting the viral PPxY-host Nedd4 interface block egress of a broad range of RNA viruses. J. Virol. 88, 7294–7306. https://doi.org/10.1128/JVI.00591-14

Harty, R.N., Brown, M.E., McGettigan, J.P., Wang, G., Jayakar, H.R., Huibregtse, J.M., Whitt, M.A., Schnell, M.J., 2001. Rhabdoviruses and the cellular ubiquitin-proteasome system: a budding interaction. J. Virol. 75, 10623–10629. https://doi.org/10.1128/JVI.75.22.10623-10629.2001

Harty, R.N., Brown, M.E., Wang, G., Huibregtse, J., Hayes, F.P., 2000. A PPxY motif within the VP40 protein of Ebola virus interacts physically and functionally with a ubiquitin ligase: implications for filovirus budding. Proc. Natl. Acad. Sci. U. S. A. 97, 13871–13876. https://doi.org/10.1073/pnas.250277297

Huang, X., Poy, F., Zhang, R., Joachimiak, A., Sudol, M., Eck, M.J., 2000. Structure of a WW domain containing fragment of dystrophin in complex with beta-dystroglycan. Nat. Struct. Biol. 7, 634–638. https://doi.org/10.1038/77923

Huelsenbeck, J.P., Ronquist, F., 2001. MRBAYES: Bayesian inference of phylogenetic trees. Bioinformatics 17, 754–755. https://doi.org/10.1093/bioinformatics/17.8.754

Iglesias-Bexiga, M., Palencia, A., Corbi-Verge, C., Martin-Malpartida, P., Blanco, F.J., Macias, M.J., Cobos, E.S., Luque, I., 2019. Binding site plasticity in viral PPxY Late domain recognition by the third WW domain of human NEDD4. Sci. Rep. 9, 15076. https://doi.org/10.1038/s41598-019-50701-3

Imseng, S., Aylett, C.H., Maier, T., 2018. Architecture and activation of phosphatidylinositol 3-kinase related kinases. Curr. Opin. Struct. Biol. 49, 177–189. https://doi.org/10.1016/j.sbi.2018.03.010

Kanelis, V., Rotin, D., Forman-Kay, J.D., 2001. Solution structure of a Nedd4 WW domain-ENaC peptide complex. Nat. Struct. Biol. 8, 407–412. https://doi.org/10.1038/87562

Lam, T.T.-Y., Shum, M.H.-H., Zhu, H.-C., Tong, Y.-G., Ni, X.-B., Liao, Y.-S., Wei, W., Cheung, W.Y.-M., Li, W.-J., Li, L.-F., Leung, G.M., Holmes, E.C., Hu, Y.-L., Guan, Y., 2020. Identifying SARS-CoV-2 related coronaviruses in Malayan pangolins. Nature. https://doi.org/10.1038/s41586-020-2169-0

Li, F., 2013. Receptor recognition and cross-species infections of SARS coronavirus. Antiviral Res. 100, 246–254. https://doi.org/10.1016/j.antiviral.2013.08.014

Li, F., 2012. Evidence for a common evolutionary origin of coronavirus spike protein receptor-binding subunits. J. Virol. 86, 2856–2858. https://doi.org/10.1128/JVI.06882-11

Lin, W., Kim, S.S., Yeung, E., Kamegaya, Y., Blackard, J.T., Kim, K.A., Holtzman, M.J., Chung, R.T., 2006. Hepatitis C virus core protein blocks interferon signaling by interaction with the STAT1 SH2 domain. J. Virol. 80, 9226–9235. https://doi.org/10.1128/JVI.00459-06

Linding, R., Jensen, L.J., Diella, F., Bork, P., Gibson, T.J., Russell, R.B., 2003. Protein disorder prediction: implications for structural proteomics. Structure 11, 1453–1459. https://doi.org/10.1016/j.str.2003.10.002

London, N., Raveh, B., Cohen, E., Fathi, G., Schueler-Furman, O., 2011. Rosetta FlexPepDock web server--high resolution modeling of peptide-protein interactions. Nucleic Acids Res. 39, W249–53. https://doi.org/10.1093/nar/gkr431

Ohya, K., Kajigaya, S., Kitanaka, A., Yoshida, K., Miyazato, A., Yamashita, Y., Yamanaka, T., Ikeda, U., Shimada, K., Ozawa, K., Mano, H., 1999. Molecular cloning of a docking protein, BRDG1, that acts downstream of the Tec tyrosine kinase. Proc. Natl. Acad. Sci. U. S. A. 96, 11976–11981. https://doi.org/10.1073/pnas.96.21.11976

Petit, C.M., Chouljenko, V.N., Iyer, A., Colgrove, R., Farzan, M., Knipe, D.M., Kousoulas, K.G., 2007. Palmitoylation of the cysteine-rich endodomain of the SARS-coronavirus spike glycoprotein is important for spike-mediated cell fusion. Virology 360, 264–274. https://doi.org/10.1016/j.virol.2006.10.034

Rius, J., Cores, F., Solsona, F., van Hemert, J.I., Koetsier, J., Notredame, C., 2011. A user-friendly web portal for T-Coffee on supercomputers. BMC Bioinformatics 12, 150. https://doi.org/10.1186/1471-2105-12-150

Robinson, J.W., Leshchyns'ka, I., Farghaian, H., Hughes, W.E., Sytnyk, V., Neely, G.G., Cole, A.R., 2014. PI4KIIα phosphorylation by GSK3 directs vesicular trafficking to lysosomes. Biochem. J 464, 145–156. https://doi.org/10.1042/BJ20140497

Strack, B., Calistri, A., Accola, M.A., Palu, G., Gottlinger, H.G., 2000. A role for

ubiquitin ligase recruitment in retrovirus release. Proc. Natl. Acad. Sci. U. S. A. 97, 13063–13068. https://doi.org/10.1073/pnas.97.24.13063

Thevenet, P., Shen, Y., Maupetit, J., Guyon, F., Derreumaux, P., Tufféry, P., 2012. PEP-FOLD: an updated de novo structure prediction server for both linear and disulfide bonded cyclic peptides. Nucleic Acids Res. 40, W288–93. https://doi.org/10.1093/nar/gks419

To, K.K.-W., Tsang, O.T.-Y., Leung, W.-S., Tam, A.R., Wu, T.-C., Lung, D.C., Yip, C.C.-Y., Cai, J.-P., Chan, J.M.-C., Chik, T.S.-H., Lau, D.P.-L., Choi, C.Y.-C., Chen, L.-L., Chan, W.-M., Chan, K.-H., Ip, J.D., Ng, A.C.-K., Poon, R.W.-S., Luo, C.-T., Cheng, V.C.-C., Chan, J.F.-W., Hung, I.F.-N., Chen, Z., Chen, H., Yuen, K.-Y., 2020. Temporal profiles of viral load in posterior oropharyngeal saliva samples and serum antibody responses during infection by SARS-CoV-2: an observational cohort study. Lancet Infect. Dis. https://doi.org/10.1016/S1473-3099(20)30196-1

Trott, O., Olson, A.J., 2010. AutoDock Vina: improving the speed and accuracy of docking with a new scoring function, efficient optimization, and multithreading. J. Comput. Chem. 31, 455–461. https://doi.org/10.1002/jcc.21334

Vaguine, A.A., Richelle, J., Wodak, S.J., 1999. SFCHECK: a unified set of procedures for evaluating the quality of macromolecular structure-factor data and their agreement with the atomic model. Acta Crystallogr. D Biol. Crystallogr. 55, 191–205. https://doi.org/10.1107/S0907444998006684

Wang, D.S., Shaw, R., Winkelmann, J.C., Shaw, G., 1994. Binding of PH domains of beta-adrenergic receptor kinase and beta-spectrin to WD40/beta-transducin repeat containing regions of the beta-subunit of trimeric G-proteins. Biochem. Biophys. Res. Commun. 203, 29–35. https://doi.org/10.1006/bbrc.1994.2144

Wirblich, C., Tan, G.S., Papaneri, A., Godlewski, P.J., Orenstein, J.M., Harty, R.N., Schnell, M.J., 2008. PPEY motif within the rabies virus (RV) matrix protein is essential for efficient virion release and RV pathogenicity. J. Virol. 82, 9730–9738. https://doi.org/10.1128/JVI.00889-08

Yang, W.C., Ching, K.A., Tsoukas, C.D., Berg, L.J., 2001. Tec kinase signaling in T cells is regulated by phosphatidylinositol 3-kinase and the Tec pleckstrin homology domain. J. Immunol. 166, 387–395. https://doi.org/10.4049/jimmunol.166.1.387

Zaidman, D., Wolfson, H.J., 2016. PinaColada: peptide–inhibitor ant colony ad-hoc design algorithm. Bioinformatics 32, 2289–2296. https://doi.org/10.1093/bioinformatics/btw133

Zhang, T., Wu, Q., Zhang, Z., 2020. Probable Pangolin Origin of SARS-CoV-2 Associated with the COVID-19 Outbreak. Curr. Biol. 30, 1346–1351.e2. https://doi.org/10.1016/j.cub.2020.03.022

FIGURES LEGEND

Figure 1. Multiple alignment of spike (S) protein of betacoronaviruses using T-coffee software. **(A)** Localization of PPxY Late domain in N-terminal. PPxY Late domain motifs are colored in blue. ^{28}YTNSF^{32} motif (green arrows), when its Tyr is phosphorylated, is able to bind Src Homology 2 (SH2) domain. GenBank and UniProt accession numbers are indicated at the start of each sequence. The figure was prepared with ESPript (http://espript.ibcp.fr). (B) Alignment of codons of PPxY motifs. If nucleotides in red mutate into cytosine it will transform codons into proline. (C) Unrooted phylogenetic tree of whole S protein sequences of representative betacoronaviruses. The tree was constructed using Mr Bayes method based on the multiple alignment of the whole S protein sequences by T-coffee. Betacoronaviruses in blue possess a PPxY motif. GenBank and UniProt accession numbers are indicated at the start of each sequence.

Figure 2. Cartoon and surface representation of human Nedd4 WW3-domain (PDBid: 2KQ0_A) with docked peptides. (A) ^{23}QL**PP**A**Y**TNS^{31} peptide of SARS-CoV-2 S protein (cyan) and (B) ^{23}QL**PP**A**Y**TNS^{31} superposed to Zaire Ebola virus Matrix protein VP40 (^{112}TA**PP**E**Y**MEA^{120}) peptide (green, PDBid: 2KQ0_B). (C) Surface representation of Nedd4 WW3-domain with peptides in sticks. Images were generated using PyMol (www.pymol.org).

Table 1. PPxY late-domain motif in single stranded enveloped RNA viruses.

Viruses	Family	disease in human	Geography	PPxY protein	Reference
HIV-1	Retroviruses	AIDS	World	Gag	Strack et al., 2000
HTLV-1	Retroviruses	Aggressive lymphoma	World	Gag	Bouamr et al., 2003
Rhabies	Rhabdoviruses	Deadly brain inflammation	World	M	Harty et al., 2001
Marburg	Filoviruses	Deadly hemorrhagic fever	West Africa	VP40	Dolnik et al., 2010
Ebola	Filoviruses	Deadly hemorrhagic fever	West Africa	VP40	Harty et al., 2000
Lassa virus	Arenaviruses	Deadly hemorrhagic fever	West Africa	Z matrix	Baillet et al., 2019

Table. 2. ELM motifs of hot disordered loop in SARS-CoV-2 S protein.

Elm Name	Instances	Positions	Elm Description	Cell compartment	Pattern
LIG_WW_1	PPAY	25-28	PPXY is the motif recognized by WW domains of Group I.	cytosol, membrane	PP.Y
LIG_SH2_STAP1	YTNSF	28-32	STAP1 Src Homology 2 (SH2) domain Class 2 binding motif.	plasma membrane	(Y)[DESTA][^GP][^GP][ILVFMWYA]
LIG_SH2_STAT5	YTNS	28-31	STAT5 Src Homology 2 (SH2) domain binding motif.	cytosol	(Y)[VLTFIC]..
MOD_GSK3_1	PAYTNSFT	26-33	GSK3 phosphorylation recognition site.	cytosol, nucleus	...([ST])...[ST]
MOD_PIKK_1	TTRTQLP	19-25	(ST)Q motif which is phosphorylated by PIKK family members.	nucleus, cytosol	...([ST])Q..

A

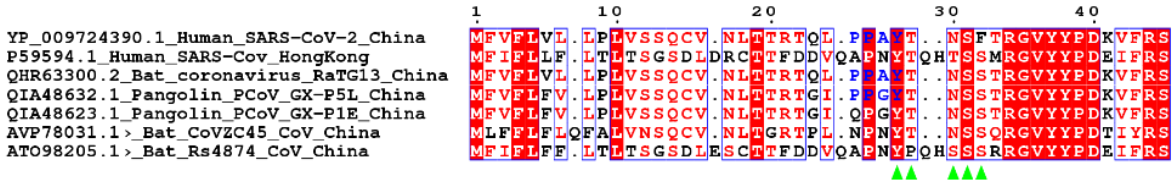
1 10 20 30 40
YP_009724390.1_Human_SARS-CoV-2_China
P59594.1_Human_SARS-Cov_HongKong
QHR63300.2_Bat_coronavirus_RaTG13_China
QIA48632.1_Pangolin_PCoV_GX-P5L_China
QIA48623.1_Pangolin_PCoV_GX-P1E_China
AVP78031.1>_Bat_CoVZC45_CoV_China
ATO98205.1>_Bat_Rs4874_CoV_China

B

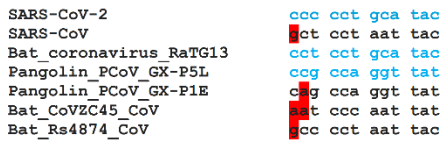
SARS-CoV-2 ccc cct gca tac
SARS-CoV gct cct aat tac
Bat_coronavirus_RaTG13 cct cct gca tac
Pangolin_PCoV_GX-P5L ccg cca ggt tat
Pangolin_PCoV_GX-P1E cag cca ggt tat
Bat_CoVZC45_CoV aat ccc aat tat
Bat_Rs4874_CoV gcc cct aat tac

C

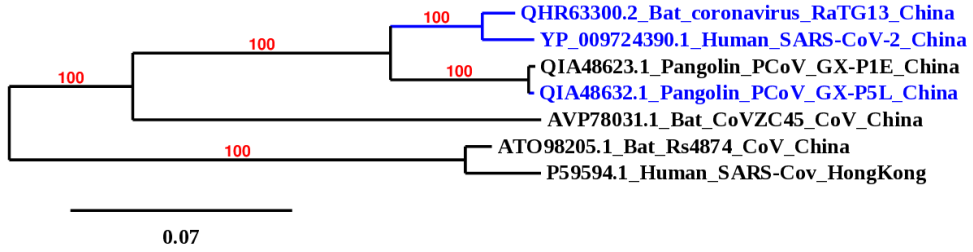
QHR63300.2_Bat_coronavirus_RaTG13_China
YP_009724390.1_Human_SARS-CoV-2_China
QIA48623.1_Pangolin_PCoV_GX-P1E_China
QIA48632.1_Pangolin_PCoV_GX-P5L_China
AVP78031.1_Bat_CoVZC45_CoV_China
ATO98205.1_Bat_Rs4874_CoV_China
P59594.1_Human_SARS-Cov_HongKong
100
100
100
100
100
0.07

Fig. 1

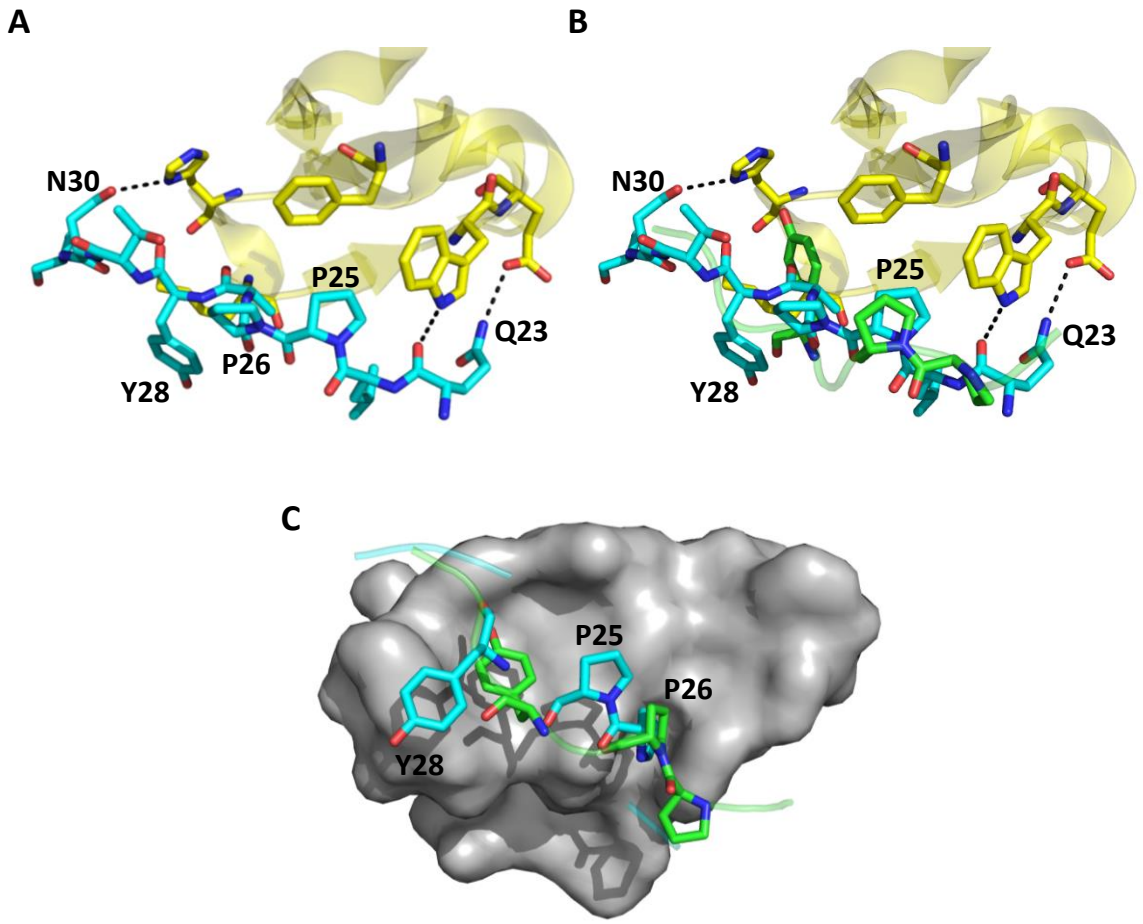

Fig. 2